Theor Chem Acc (2007) 117:793–803
DOI 10.1007/s00214-006-0205-2

REGULAR ARTICLE

A test case for time-dependent density functional theory calculations of electronic circular dichroism: 2-chloro-4-methoxy-6-[(R)-1-phenylethylamino]-1,3,5- triazine

Giuliano Alagona · Caterina Ghio · Susanna Monti

Received: 13 June 2006 / Accepted: 13 October 2006 / Published online: 5 January 2007
© Springer-Verlag 2007

Abstract The three-dimensional structure of an optically active substituted s-triazine derivative, 2-chloro-4-methoxy-6-[(R)-1-phenylethylamino]-1,3,5-triazine, has been studied by conformational analysis using density functional theory (DFT) both in vacuo and in acetonitrile solution in the polarizable continuum model integral equation formalism framework. Time-dependent DFT methods have been used to investigate the molecular electronic CD and absorption UV spectra. Comparison with experimental results allowed the reliability of the theoretical predictions to be enhanced and suggested a possible interpretation of the measured data.

Keywords Spectroscopic properties · PCM · mPW1PW91 · BH&HLYP · CD spectra · DeVoe model

1 Introduction

The optical properties of chiral molecules are extremely interesting and of paramount importance especially for compounds of pharmacological relevance. The absolute configuration of a chiral molecule can in principle be obtained from measurement of electronic circular dichroism (CD) which is defined as the differential absorption of left and right handed circularly polarized light [1,2]. Indeed, CD spectroscopy is one of the most widely used methods in chiral spectroscopy and it has proven to be a powerful technique in the determination of the prevailing conformation in solution of various optically active compounds [3]. However, the simultaneous use of experimental methods and theoretical predictions enhance the reliability of the obtained results and facilitate their interpretation [4–6]. CD sensitivity to molecular 3D-geometries and to their corresponding electronic structures requires a highly accurate theoretical treatment. Among the various computational techniques, modern time dependent density functional theory (TDDFT) methods have been found to be trustworthy and have been successfully applied to the calculation of electronic CD [7,8]. Nonetheless, the theoretical prediction of experimental electronic CD spectra is a very arduous task. In fact, an accurate quantum chemical description of the excitation energies non necessarily provides correspondingly accurate rotatory strengths, which represent the main signed quantity in CD spectroscopy. Moreover, when there are no data providing experimental values for the relative energies of the conformations a molecule can take, percentage populations necessary to obtain spectra comparable to experiment must be estimated using theoretical methodologies which exhibit limitations, due to their intrinsic approximations.

In the present study, TDDFT methods are used to investigate the molecular electronic CD and absorption UV spectra of 2-chloro-4-methoxy-6-[(R)-1-phenylethylamino]-1,3,5-triazine (TRI), an optically active substituted s-triazine derivative (synthesized by the group of P. Salvadori at the University of Pisa) which belongs to

Electronic supplementary material The online version of this article (doi:10.1007/s00214-006-0205-2) contains supplementary material, which is available to authorized users.

G. Alagona · C. Ghio (✉) · S. Monti
Molecular Modeling Lab., Istituto per i Processi Chimico-Fisici (IPCF-CNR), Via G. Moruzzi 1, 56124 Pisa, Italy
e-mail: C.Ghio@ipcf.cnr.it

S. Monti (✉)
e-mail: S.Monti@ipcf.cnr.it

an appealing class of chiral solvating agents (CSAs) for NMR spectroscopy and can be used either to prepare chiral stationary phases (CSPs) for HPLC or as CSA. A similar compound, (+)-2-[(R)-1-(9-anthryl)ethylamino]-4-chloro-6-methoxy-1,3,5- triazine (ARY), which possesses the 1-arylethylamino group in place of the 1-phenylamino moiety, was previously synthesized and studied, using UV, CD and NMR spectroscopies, by the aforementioned team which succeeded in elucidating the conformation taken by that molecule in solution [9,10]. Unfortunately, the application of the same methodologies to the TRI compound did not produce favorable results due to its greater flexibility. In particular neither reliable NMR nor IR/Raman data are available, thus conformational populations have not been experimentally determined.

2 Computational details

Density functional theory calculations, using both the Becke three-parameter hybrid functional in conjunction with the Lee–Yang–Parr correlation functional (B3LYP) [11,12] and the BH&HLYP functional [12–14] with Pople's standard 6-31G* basis set, were applied to fully optimize TRI geometries in vacuo and in acetonitrile solution. Frequency calculations were carried out to confirm the conformational stationary points. Solvent effects were introduced through a continuum approach represented by the integral equation formalism (IEF) [15–17] version of the polarizable continuum model (PCM) [18,19]. The molecular cavity was obtained in terms of interlocking spheres centered on oxygen, carbons, nitrogens, amidic hydrogen (using Bondi radii [20]), while for methyl groups and CH groups a united atom description has been used. The chosen radii [R(O)=1.52 Å, R(C)=1.70 Å, R(N)=1.55 Å, R(CH_3)=2.00 Å, R(CH)=1.90 Å and R(H)=1.2 Å] were multiplied by a cavity-size factor equal to 1.2 [21,22]. All the calculations were performed using the Gaussian 03 computer code [14]. Thermal corrections for obtaining standard relative internal free energies, for the selected conformers, were calculated in the rigid-rotator, harmonic oscillator approximation [23] only at the B3LYP/6-31G* level.

Electronic excitation spectra (UV) and Circular Dichroism spectra (CD) of TRI were calculated at the density functional level using the time dependent perturbation theory approach (TDDFT), in which excited-state properties are determined from the linear response of the molecules to an external continuous wave field, by using a more extended basis set, i.e. 6-311++G(d,p). A combination of hybrid functionals differing in a fraction of *exact* Hartree–Fock exchange (HFXC) with a large basis set augmented with diffuse functions, is highly recommended [7,24] to obtain results able to satisfactorily reproduce the experimental data. The UV spectra were simulated by overlapping Gaussian functions with a full width of 0.17 eV at the 1/e of the maximum for each calculated electronic transition. The vibrational broadening of the experimental CD bands was simulated by summing rotatory strengths (R, in the origin invariant velocity gauge formulation) weighted gaussian curves with a full width of 0.17 eV at the 1/e of the maximum for each calculated electronic transition.

Theoretical UV and CD spectra were also obtained using the classical physics approach developed by DeVoe [25–27] which succeeded in reproducing satisfactorily the experimental spectra of a large variety of different molecular systems [3]. The allowed transitions of each chromophore were described in terms of dipoles located in the center of the rings, having a dipolar strength calculated from experimental UV spectra of suitable model compounds. Two dipoles located in the center of each ring and directed perpendicularly to each other were used to describe the electrically allowed transitions of the triazine and benzene chromophores with dipolar strengths of 10 D^2 and 20 D^2 centered at 225 and 185 nm, respectively, to reproduce the observed UV intensities [28].

3 Results and discussion

3.1 Conformational analysis

In order to find the most stable conformers of TRI, a systematic conformational search of the potential energy surface (PES) was carried out at the B3LYP/6-31G* level of theory. Two main degrees of conformational freedom were identified: the rotamerism around the N_{NH}–C_{chiral} bond described by the dihedral angle τ_1 and the rotamerism around the C_{chiral}–C_{phenyl} bond described by the dihedral angle τ_2 (Fig. 1). In order

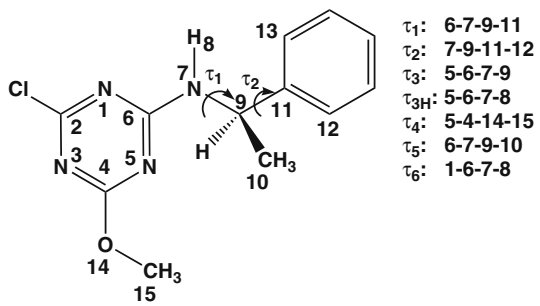

Fig. 1 2-chloro-4-methoxy-6-[(R)-1-phenylethylamino]-1,3,5-triazine (TRI) structure

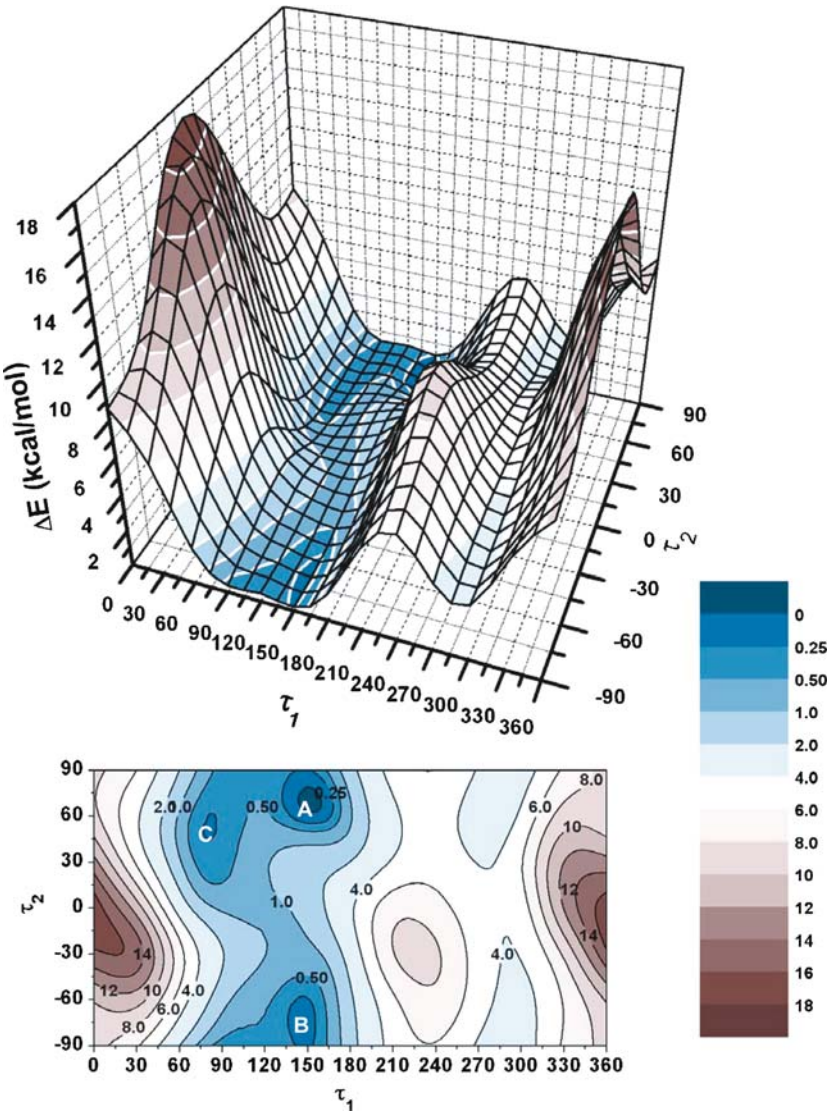

Fig. 2 B3LYP/6-31G* τ_1, τ_2 potential energy surface for $\tau_6 = 0°$ (**1**) TRI

to perform an accurate investigation of the conformational landscape, the PES for pairs of τ_1, τ_2 values was examined for either the $\tau_6 = 0°$ (**1**) and $\tau_6 = 180°$ (**2**) arrangements. The conformations were generated by rotating both the τ_1 and τ_2 angles from 0° to 180° in 30° increments. The conformational search procedure is not exhaustive but should give a fair representation of possible TRI conformations. Inspection of the PES maps (one of them (**1**) is reported in Fig. 2) permitted the identification of three stable conformations, namely **A**, **B** and **C**, for each value of the τ_6 torsion angle, located respectively at $\tau_1 \approx 150°/\tau_2 \approx 60°, \tau_1 \approx 150°/\tau_2 \approx -60°$, and $\tau_1 \approx 80°/\tau_2 \approx 50°$. These structures, six in all, were further fully optimized at the B3LYP/6-31G* level and at the BH&HLYP/6-31G* level without any constraint both in the gas phase and in acetonitrile solution, using IEF-PCM, and frequency calculations were performed on the obtained rotamers to confirm that these conformations were true minima. Geometrical parameters and energy differences are summarized in Tables 1, 2 and 3. The relative energies and free energies of the six conformers (whose structures are displayed in Fig. 3) were calculated in vacuo and in acetonitrile solution both at the B3LYP/6-31G* and BH&HLYP/6-31G* level including zero point energy (ZPE) contributions obtained from frequency analysis. Final free energies in acetonitrile include both electrostatic and non electrostatic contributions (i.e. dispersion, repulsion and cavitation terms). The reported values do not contain thermal corrections, to avoid problems due to hindered rotations. In order to distinguish between the various quantities, ΔE (or ΔG) has been used when ΔZPE corrections are included. For all conformations, percentage populations were calculated on the basis of relative energy and free energy values using Boltzmann statistics at $T = 298$ K. The final optimized conformations obtained using the

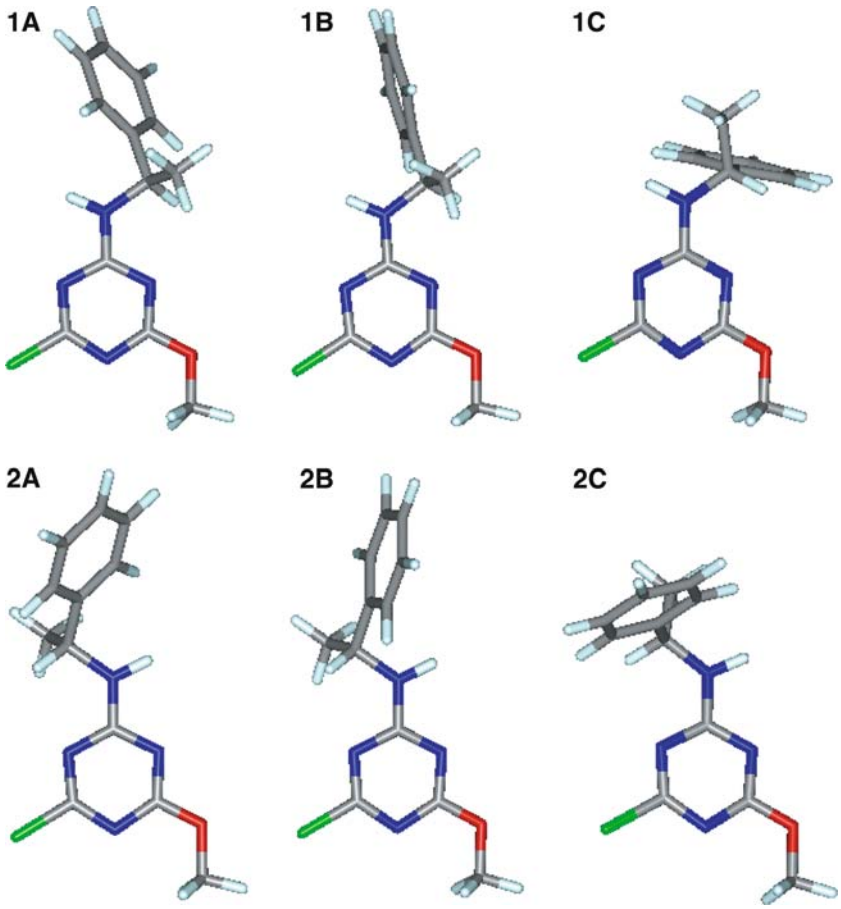

Fig. 3 B3LYP/6-31G* structures of local minima on the PES fully optimized without any constraint in acetonitrile solution using the PCM method

Table 1 Dihedral angles (degrees) of the B3LYP/6-31G* optimized geometries in the gas phase (vac) and in acetonitrile solution (sol)

mol	τ_1		τ_2		τ_3		τ_{3H}		τ_4		τ_5	
	vac	sol	vac	sol	vac	sol	vac	sol	vac	sol	vac	sol
1A	154.7	151.5	65.2 −114.6	64.8 −115.2	2.8	−0.7	177.2	−179.8	179.9	180.0	−79.9	−83.2
1B	149.2	146.1	−71.2 107.9	−74.3 104.9	−1.7	−2.8	−178.4	−177.5	179.9	179.7	−82.9	−86.2
1C	81.4	86.6	61.2 −119.3	40.1 −143.1	7.4	1.6	175.7	179.4	−179.7	179.9	−153.2	−149.3
2A	154.2	148.7	65.8 −113.9	68.4 −111.3	−177.5	178.8	−2.3	1.6	179.8	179.8	−80.4	−85.6
2B	149.3	146.2	−69.9 109.4	−71.4 108.0	177.7	177.7	2.4	2.3	179.9	179.8	−82.9	−86.2
2C	81.3	83.2	60.2 −120.4	44.5 −138.0	−173.1	−176.6	−4.9	−1.8	179.8	180.0	−153.4	−152.6

two different functionals were structurally very similar having root mean square deviations lower than 0.01 Å.

On closer examination of the reported results it appears that the minimum energy structures can be subdivided into two distinct types, namely, extended geometries (***e***), comprising structures **A** and **B**, and folded geometries (***f***), comprising structure **C**, which are characterized by a different distance between the ring moieties and peculiar values of the torsion angles.

Type ***e*** structures (**A** and **B** conformers) have wider centroid ring separations (d ≈ 6.2 Å) (see Table 2) and *extended* conformations with almost equal $\tau_1, \tau_3, \tau_{3H}, \tau_4$ and τ_5 dihedral angles with a maximum difference of about 5.5° (observed for τ_1), but a distinct arrangement

Table 2 Relative stabilities (kcal/mol), percentage populations (%) and centroid ring distances (d in Å) of the B3LYP/6-31G* optimized geometries in the gas phase (vac) and in acetonitrile solution (sol)

mol	vac					sol				
	ΔE	%	ΔE	%	d	ΔG	%	ΔG	%	d
1A	0.00	25.9	0.00	27.7	6.2	0.00	23.4	0.02	23.4	6.2
1B	0.23	17.6	0.33	15.7	6.2	0.19	17.0	0.29	14.8	6.1
1C	0.22	17.9	0.27	17.4	5.2	0.07	20.8	0.00	24.0	5.4
2A	0.28	16.2	0.28	17.2	6.2	0.16	18.0	0.18	17.6	6.2
2B	0.51	10.9	0.61	10.0	6.2	0.56	9.1	0.65	8.0	6.1
2C	0.48	11.5	0.49	12.0	5.2	0.41	11.7	0.40	12.2	5.3

Table 3 Relative stabilities (kcal/mol), percentage populations (%) and centroid ring distances (d in Å) of the BH&HLYP/6-31G* optimized geometries in the gas phase (vac) and in acetonitrile solution (sol)

mol	vac					sol				
	ΔE	%	ΔE	%	d	ΔG	%	ΔG	%	d
1A	0.00	26.6	0.00	26.2	6.2	0.15	21.6	0.00	29.7	6.2
1B	0.21	18.6	0.26	16.8	6.2	0.47	12.4	0.29	18.3	6.1
1C	0.24	17.8	0.19	19.1	5.2	0.00	27.6	0.29	18.2	5.4
2A	0.33	15.2	0.31	15.4	6.2	0.46	12.7	0.34	16.8	6.2
2B	0.54	10.7	0.61	9.4	6.2	0.79	7.3	0.88	6.7	6.1
2C	0.52	11.1	0.41	13.1	5.2	0.24	18.4	0.63	10.3	5.3

of the phenyl ring system (τ_2), which in conformer **A** is rotated by about 40° with respect to the ring plane of the other structure (conformer **B**). Type ***f*** structures (**C**) have instead a somewhat shorter centroid ring distance (d ≈ 5.2 Å) and appear as *folded* geometries, where the τ_1 dihedral angle is by about 73.0° smaller than the corresponding value measured in structure **A**.

Optimization in solution of type ***e*** structures does not change substantially the torsion parameter examined (maximum $\Delta\tau \approx 5.5°$) and centroid ring distances are maintained. Major variations are observed instead for type ***f*** structures, where the maximum $\Delta\tau$ is about 24.0° ($\Delta\tau_2$) and the rings are farther apart.

The computed energy and free energy differences at the B3LYP level do not exceed 0.7 kcal/mol for a given conformer. The in vacuo relative free energy of both **1** and **2** isomers is, in the best case, ≈ 0.28 kcal/mol, whereas in acetonitrile solution the lowest relative free energy difference is ≈ 0.18 kcal/mol, thus suggesting that solvation has a small effect on the isomeric composition, continuing to favor the **1** arrangement. The effect is limited and can be ascribed to the slightly different polarity of the two isomers: more polar structures (**1**) are significantly stabilized by a relatively polar solvent such as acetonitrile. The in vacuo computed energy and free energy differences at the BH&HLYP level are very similar to the B3LYP ones whereas in acetonitrile solution both energy differences are greater with a maximum of about 0.9 kcal/mol found for structure **2B**. However, also at this level, type **1** structures are favored and conformer **1A** is recognized by both functionals as the most stable geometry. The small variation of the percentage population values in solution clearly confirms the coexistence, at room temperature, of the whole set of conformations. For this reason, there should be a remarkable contribution of each structure to the chiroptical properties of the bulk compound. However, it should be noticed that arrangements of type **1** are preferred.

3.2 Computed and experimental UV and CD spectra

3.2.1 General considerations

In order to test which combination of functional-basis set would produce acceptable UV and, primarily, CD spectra for the system under investigation when compared to the experimental data [28], excited state calculations based upon the ground state optimized geometries in vacuo of the six single conformations were performed using the time dependent DFT method with three different functionals, namely, B3LYP, mPW1PW91 [29,30] and BH&HLYP, which have an increasing fraction of HFXC (20, 25 and 50%, respectively) and two different basis sets, namely, 6-311++G** and aug-cc-pVDZ [31]. In particular, the accuracy of B3LYP and aug-cc-pVDZ in predicting optical rotations has been thoroughly documented even for compounds of remarkable size [7]. The mPW1PW91 hybrid functional has been chosen because it generally provides results which are close or even better than those obtained with the B3LYP method for a wide variety of molecular systems both at the ground and excited states [29,30,32,33].

Rotatory strengths are the main signed quantities determining the intensity of CD absorption bands, which can be positive or negative signals. CD spectra are rather sensitive to molecular details such as geometric and electronic features and the excitation energies must be known with a higher accuracy than in UV spectroscopy to avoid an incorrect cancellation of neighboring bands with opposite sign. Therefore, an accurate prediction of rotatory strengths represents a significantly more demanding task than the calculation of oscillator strengths.

From the comparison of the B3LYP simulated CD spectra computed with basis sets of different quality (Fig. 4) it was evident that, although the rotatory strengths of individual transitions could deviate considerably, the shape of the entire spectra was rather insensitive to the basis set size. Consequently the 6-311++G** basis set was considered well suited for

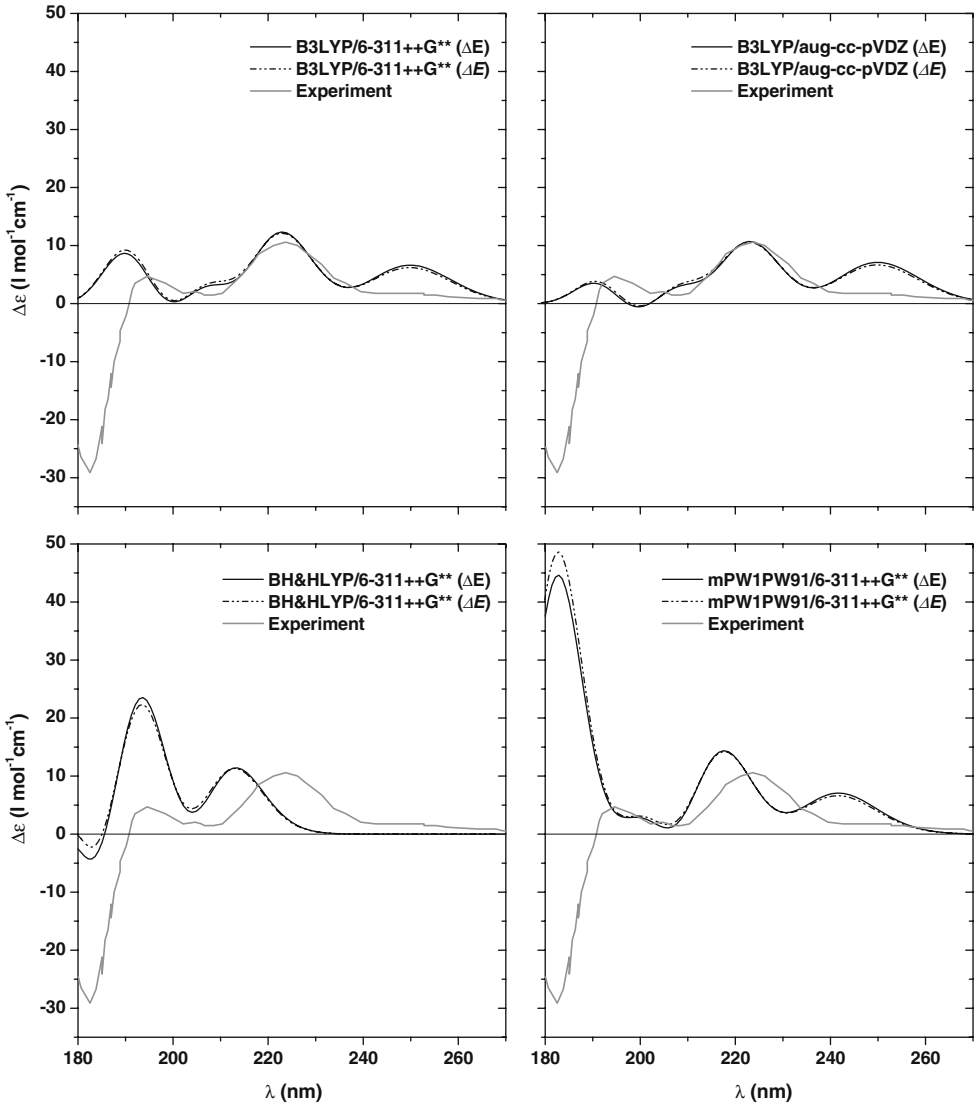

Fig. 4 Comparison of the resulting conformationally averaged theoretical CD spectra, using ΔE and Δ*E* based populations (see *legend*), in the gas phase, and the experimental CD spectrum [28]

an accurate description of CD and UV spectra of TRI rotamers and was chosen for calculations in acetonitrile solution, at the BH&HLYP level in vacuo and in acetonitrile solution, as well as for testing the mPW1PW91 hybrid functional in the gas phase.

3.2.2 UV absorption spectra

The experimental UV spectrum (displayed in Fig. 5), measured in acetonitrile solution, exhibits three significant features: the benzene-like band at about 260 nm, the s-triazine absorption band between 205 and 245 nm and a strong band with a maximum at about 190 nm attributable to the electrically allowed transition of the benzene chromophore. These features, which originate from transitions between orbitals localized on either the benzene ring or the triazine moiety, indicate that the two chromophores, that is the benzene derivative and the triazine group, are weakly coupled. Figure 6 shows the calculated UV absorption spectra of the six conformers under examination in vacuo and in acetonitrile solution using the aforementioned functionals and basis sets. From the comparison between B3LYP and mPW1PW91 calculations in vacuo a fair agreement in the reproduction of the band structure is put forward. The intensities of the identified transitions are similar indeed, whereas the energetic positions of mPW1PW91 excitations are slightly blue shifted by about 8 nm with respect to the B3LYP ones. The band structure is well reproduced by the BH&HLYP functional too, which displays more intense peaks blue shifted with respect to the B3LYP ones by about 22 nm on the average (standard deviation $\approx \pm 6$ nm). Calculations in acetonitrile solution, conversely, give rise to UV absorption spectra that differ, both in the position and intensity of the three main peaks, from those obtained through calculations in the

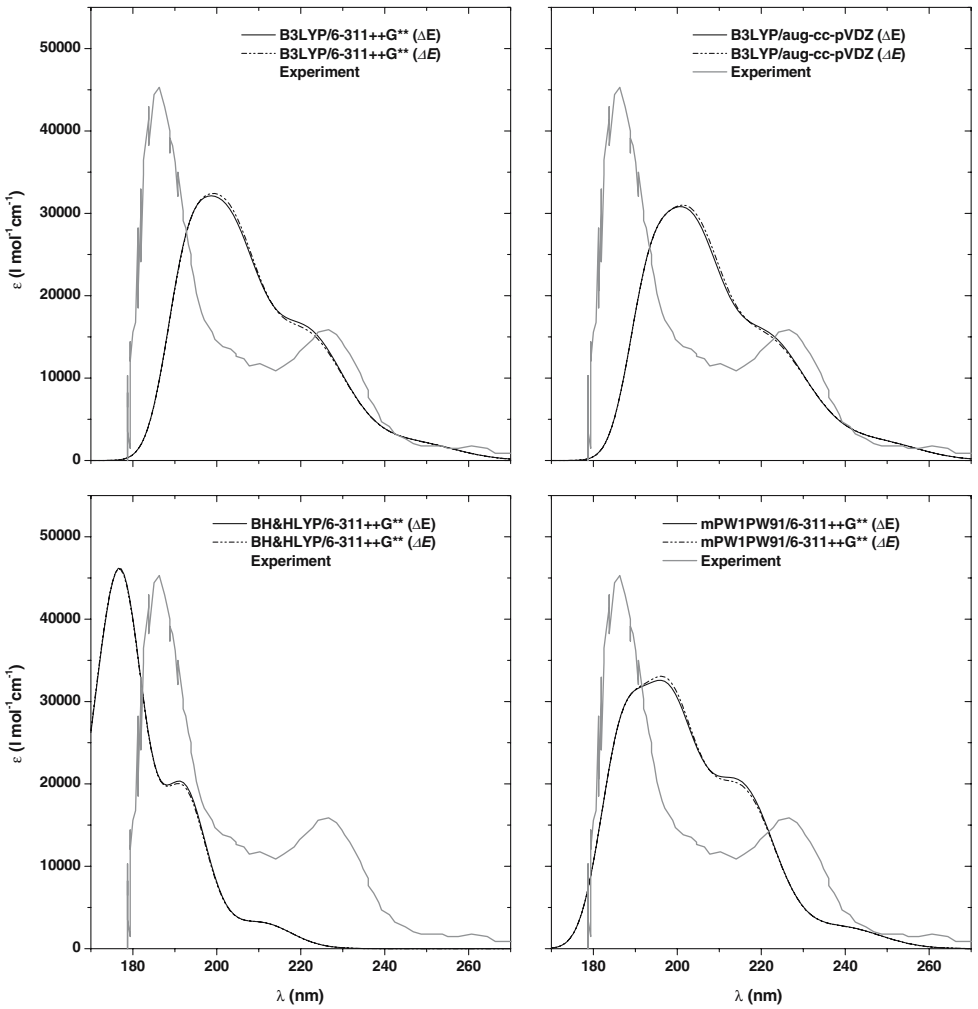

Fig. 5 Comparison of the resulting conformationally averaged theoretical UV spectra, using ΔE and Δ*E* based populations (see *legend*), in the gas phase, and the experimental UV spectrum [28]

gas phase. An increase in their height and a shift of their center to shorter wave-length values are observed with the B3LYP functional, while with the BH&HLYP one, a smaller shift of the peak centers at longer wave-length is noticed, although also in this case the heightening peak effect is present. However, all the spectra closely resemble each other exhibiting a similar band structure consistent with experimental data.

Comparison to experiment requires calculation of conformationally averaged spectra, weighting the contribution of each conformer by its fractional population. Conformational populations obtained from relative energy and free energy values using Boltzmann statistics were both taken into consideration to compare the averaged computed UV spectra in the gas phase (Fig. 5). It can be noticed that all the theoretical spectra are shifted with respect to experiment and the peak intensities do not exactly match the experimental findings. The experimental excitation at 225 nm is blue shifted in all the simulated spectra by about 9 nm with only a remarkable exception represented by the TD-BH&HLYP/6-311++G** spectrum, where the wave-length difference is about 34 nm. As far as the first peak position is concerned, a red shift by about 15 nm in the case of TD-B3LYP/6-311++G** and TD-B3LYP/aug-cc-pVDZ calculations, and by 10 nm for TD-mPW1PW91/6-311++G** is noticed. On the contrary, an opposite displacement, that is a blue shift, by about 9 nm appears in the case of the TD-BH&HLYP/6-311++G** spectrum. Despite conformer populations derived from B3LYP/6-31G* and BH&HLYP/6-31G* Δ*E* values might be not accurate enough, the resulting spectra agree satisfactorily with those generated employing populations calculated from conformational free energy differences. Thus all subsequent weighings will be performed using ΔE based values. Unfortunately, conformational populations have not been determined experimentally, thus their values must be predicted through calculations taking into account the uncertainties due to the selected methodology. The computed Boltzmann weighted UV spectra in vacuo and in acetonitrile solution, calculated using in solution optimized structures, together with the experimental counterpart taken from Ref. [28], are shown in Fig. 7 for the TD-B3LYP, TD-BH&HLYP and

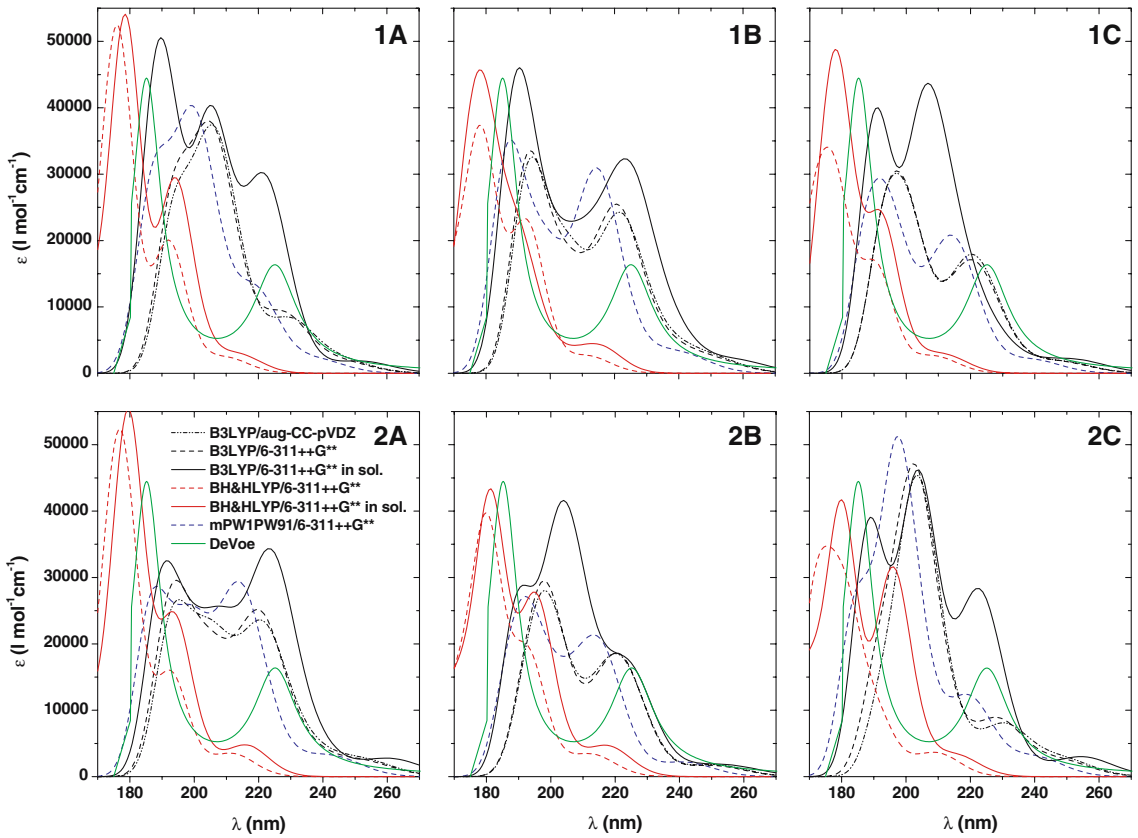

Fig. 6 Calculated UV absorption spectra of the six B3LYP/6-31G* minimum energy conformers in vacuo and in acetonitrile solution (see *legend*) using different functionals (B3LYP, BH&HLYP and mPW1PW91) and basis sets (6-311++G** and aug-cc-pVDZ). UV spectra calculated by means of DeVoe's approach are also shown

DeVoe levels of theory. The striking similarity of the Boltzmann weighted spectrum obtained through the DeVoe approach with the experimental data confirms the validity of the spectroscopic parameters chosen for DeVoe calculations, that is dipoles location, orientation and strength. As far as the other theoretical spectra are concerned, it can be noticed that TD-B3LYP calculations in acetonitrile solution lead to a theoretical spectrum which is better distributed than those at the other levels of theory although the centers of the theoretical peaks are shifted by about ±5 nm in solution (±10 nm in the gas phase) and their intensities do not exactly match the experimental findings. TD-BH&HLYP UV spectrum in solution has the correct three band shape but the transition wave-lengths are all blue shifted with respect to the experimental ones, albeit slightly less than those in vacuo.

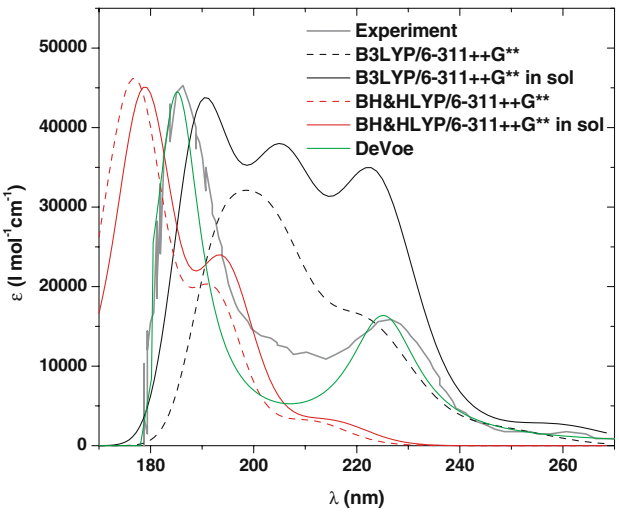

Fig. 7 Comparison of the theoretical conformationally averaged UV spectra, using ΔG and ΔE based populations (see *legend*) either in acetonitrile solution or in the gas phase, and the experimental UV spectrum

3.2.3 CD spectra

The experimental CD spectrum, measured in acetonitrile solution, is displayed in Fig. 4 together with the averaged theoretical spectra computed in vacuo. The measured CD spectrum shows two Cotton effects having opposite sign: the first one at about 225 nm ($\Delta\epsilon = +10$) and the second one at about 185 nm ($\Delta\epsilon = -30$), which

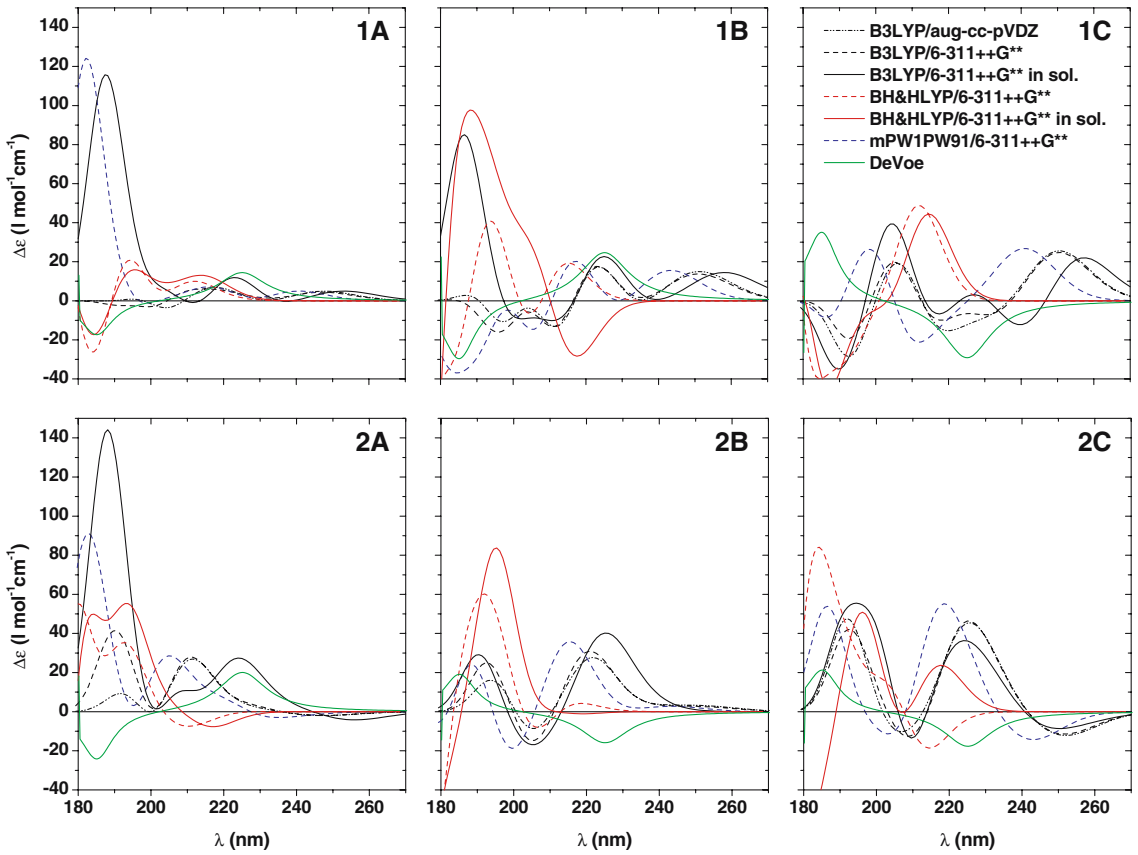

Fig. 8 Calculated CD spectra of the six B3LYP/6-31G* minimum energy conformers in vacuo and in acetonitrile solution (see *legend*) using different functionals (B3LYP, BH&HLYP and mPW1PW91) and basis sets (6-311++G** and aug-cc-pVDZ). CD spectra calculated by means of DeVoe's approach are also shown

are the two components of an exciton couplet due to coupling of the electrically allowed transitions of the benzene and s-triazine chromophores. However, it is to be taken into account that the border regions of the spectrum are not completely reliable, because wavelength data below 190 nm represent a practical limit on conventional CD instruments, such as the one employed to record the CD spectrum of the compound examined in this work (Jasco J-600 spectropolarimeter) [34]. Therefore, the attention has been concentrated on the central region of the spectrum, that is in the range between 180 and 250 nm. In Fig. 8 the simulated CD spectra of the six conformers are shown. All TD-B3LYP CD curves in acetonitrile solution show a positive long-wavelength peak at about 225 nm, which is instead shifted to shorter wavelengths when the calculations are carried out in the gas phase using either the B3LYP or the mPW1PW91 functional. Increasing HFXC to 50% causes a shift of the aforementioned transition toward a higher energy region and negative peaks, in solution, appear in the case of **1B** and **2A** structures. **1B** peak sign is altered by solvent effects, it is in fact positive in the gas phase and negative in solution. At short wavelengths, TD-B3LYP spectra in solution show a well defined peak, whose sign depends on the conformer structure. A positive sign is taken in the case of **1A**, **1B**, **2A**, **2B**, **2C** conformations, whereas for conformer **1C** the sign is inverted. Furthermore, in the case of **1B** spectrum, the peak sign is again altered by solvent effects (it is negative in the gas phase and positive in solution).

According to the DeVoe calculations, structures **1A**, **1B** and **2A** have positive couplets, whereas structures **1C**, **2B** and **2C** have negative couplets all with comparable intensities, thus an appropriate combination is necessary to reproduce the experimental spectrum. Combined spectra in the gas phase, obtained using four different levels of theory, are reported in Fig. 4, where a direct comparison with the experimental CD spectrum is also proposed. On Boltzmann averaging over the six conformations using B3LYP/6-31G* and BH&HLYP ΔE based or ΔE based populations, CD spectra of almost identical shape are predicted. In the region between 245 and 270 nm the main contribution to the B3LYP and mPW1PW91 resulting spectra is due to **1A**, **1B**, **1C** and **2B**, which have predominantly positive rotatory strengths and represent about 60% of the entire

population; on the contrary, no band structure is visible at the BH&HLYP level. In the range between 210 and 240 nm, most of the CD spectra show a positive band on Boltzmann averaging. These bands add up, thus producing a positive medium intensity peak in agreement with experimental observations. Concerning the border region, where the modeling was not as accurate because of the uncertainty in the experimental spectrum, substantial differences between predicted and observed peaks are noticed in the 180 and 205 nm range, where the positive high peaks of the **1A**, **1B**, **2A**, **2B**, **2C** conformer spectra are summed up to produce an intense positive band that in the experimental spectrum has, instead, the opposite sign such as in the spectrum obtained at the BH&HLYP level that is shifted to higher energy values.

The computed Boltzmann-weighted CD spectra in the gas phase are compared with those found in acetonitrile solution in Fig. 9. Even though the B3LYP in vacuo spectrum fits very well the experimental shape in the wavelength range between 200 and 260 nm, at shorter wavelength it fails to reproduce the experimental curve, having a positive medium intensity band. A more satisfactory agreement with experimental data is found for the BH&HLYP averaged spectrum in acetonitrile solution. The correlation applies to wavelength rotatory strengths in the range 180–240 nm, which show, however, a 9 nm shift and a somewhat overestimated magnitude. The DeVoe model succeeded in reproducing quite well the main features of the experimental CD spectrum, that is correct sequence of band signs and magnitude of their intensity.

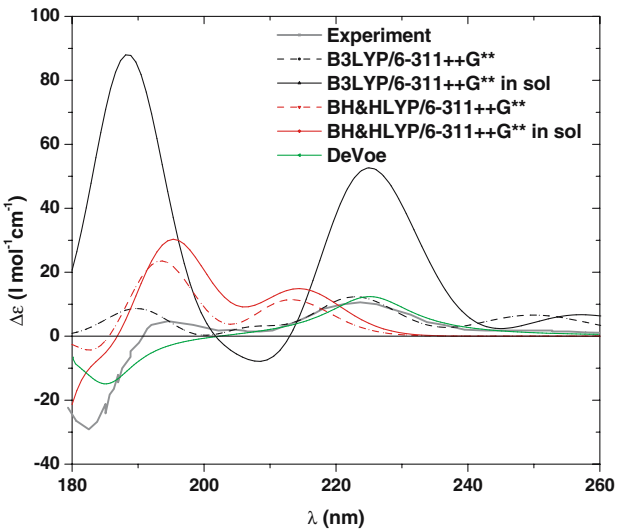

Fig. 9 Comparison of the theoretical conformationally averaged CD spectra, using ΔG and ΔE based populations (see *legend*) either in acetonitrile solution or in the gas phase, and the experimental CD spectrum

4 Conclusions

The theoretical UV and CD spectra reproduce the major features of the experimental spectra of 2-chloro-4-methoxy-6-[(R)-1-phenylethylamino]-1,3,5-triazine (TRI) quite well. Discrepancies are largely attributable to the assigned arbitrary band widths of the gaussian band shapes assumed to replicate the measured data and the functional chosen to calculate single conformer spectra. The results obtained at the B3LYP/6-31G* and BH&HLYP/6-31G* levels indicate that the isolated TRI molecule might exist in six different conformations. These structures can be grouped into two distinct families, corresponding to *folded* and *extended* conformations, on the basis of the mutual position of their ring systems.

The individual conformer spectra do not reveal all the characteristic bands present in the experimental spectrum, which, on the contrary, can be satisfactorily reproduced by an appropriate combination of them. Thus, it can be inferred that more than one conformer is present in acetonitrile solution.

This investigation has disclosed two main important aspects. (1) The CD spectra of TRI obtained by TD-DFT computations depend crucially on the selected functional. Not all the considered functionals predict correctly the sign of the investigated transitions and differences are observed in the calculated excitation energies. Despite B3LYP and mPW1PW91 are largely used and provide good results for a wide variety of chemical systems, they do not succeed, in the case of TRI, in reproducing the experimental CD spectrum, predicting an incorrect sign of the transitions around 185 nm. Their similar behavior is probably attributable to the similar amount of HFXC they contain, in fact, increasing HFXC to 50%, an improvement in the prediction is achieved. These findings suggest that the encountered difficulties in reproducing the experimental data are mainly due to fundamental deficiencies of the models. The importance of the HFXC is demonstrated by the better performance of BH&HLYP, which yields results in closer agreement with experiment than the other functionals, although deviations still remain. (2) Even though a better quantitative agreement is obtained using the DeVoe approach, a correct knowledge of TRI conformers and their concentration is necessary. A reliable conformational analysis procedure to determine the structure of conformers and, above all, their distribution, is critical for a satisfactory reproduction of the experimental spectra, especially in those cases, such as this one, where multiple minima are present and give CD couplets with comparable intensity but different sign.

Theoretical data indicate that the conformational and chiroptical properties of flexible molecules such as TRI, which exhibit multiple conformers, are not only intimately dependent on the interplay of interactions related to the type and position of their various groups, but also on the populations of their conformers.

Acknowledgments The authors thank Anna Iuliano (Dipartimento di Chimica e Chimica Industriale, Università degli Studi di Pisa) for stimulating their interest in TRI.

Electronic supplementry material

Tables with geometries, excitation energies, rotatory and oscillator strengths for all the conformations calculated at the B3LYP/6-311++G** and at the BH&HLYP/6-311++G** level in acetonitrile solution are reported.

References

1. Nakanishi K, Berova N, Woody RW (eds) (1994) Circular dichroism. VCH Publishers, New York
2. Lightner DA, Gurst JE (2000) Organic conformational analysis and stereochemistry from circular dichroism spectroscopy. Wiley-VCH, New York
3. Superchi S, Giorgio E, Rosini C (2004) Chirality 16:422–451
4. Pescitelli G, Berova N, Xiao TL, Rozhkov RV, Larock RC, Armstrong DW (2003) Org Biomol Chem 1:186–190
5. Tanaka K, Pescitelli G, Di Bari L, Nakanishi TLXK, Armstrong DW, Berova N (2004) Org Biomol Chem 2: 48–58
6. Alagona G, Ghio C, Iuliano A, Monti S, Pieraccini I, Salvatori P (2003) J Org Chem 68:3145–3157
7. Stephens PJ, McCann DM, Devlin FJ, Cheeseman JR, Frisch MJ (2004) J Am Chem Soc 126:7514–7521
8. Diedrich C, Grimme S (2003) J Phys Chem A 107:2524–2539
9. Iuliano A, Voir I, Salvadori P (1999) J Org Chem 64:5754–5756
10. Iuliano A, Uccello-Barretta G, Salvadori P (2000) Tetrahedron Asymmetry 11:1555–1563
11. Becke AD (1988) Phys Rev A 38:3098–3100
12. Lee C, Yang W, Parr RG (1988) Phys Rev B 37:785–789
13. Becke AD (1993) J Chem Phys 98:1372
14. Frisch MJ et al (2003) Gaussian 03, Revision A.1. Gaussian, Inc., Pittsburgh
15. Cancès E, Mennucci B (1998) J Math Chem 23:309–326
16. Cancès E, Mennucci B, Tomasi J (1997) J Chem Phys 107:3032–3041
17. Mennucci B, Cancès E, Tomasi J (1997) J Phys Chem B 101:10506–10517
18. Miertus S, Scrocco E, Tomasi J (1981) Chem Phys 55:117–129
19. Cammi R, Tomasi J (1995) J Comp Chem 16:1449–1458
20. Bondi A (1964) J Phys Chem 68:441–451
21. Tomasi J, Persico M (1994) Chem Rev 94:2027–2094
22. Tomasi J, Mennucci B, Cammi R (2005) Chem Rev 105:2999–3094
23. McQuarrie DA (2000) Statistical mechanics. University Science Books, Sausalito, CA
24. Stephens PJ, McCann DM, Butkus E, Stonius S, Cheeseman JR, Frisch MJ (2004) J Org Chem 69:1948–1958
25. DeVoe H (1964) J Chem Phys 41:393
26. DeVoe H (1965) J Chem Phys 43:3199
27. Rosini C, Zandomeneghi M, Salvadori P (1993) Tetrahedron Asymmetry 4:545
28. Voir I (1998) Sintesi di nuovi ausiliari chirali a struttura 1,3,5-triazinica e loro impiego per la determinazione dell'eccesso enantiomerico mediante HPLC e NMR. Thesis, Università degli Studi di Pisa
29. Adamo C, diMatteo A, Barone V (1999) From classical density functional to adiabatic connection methods. The state of the art, vol 36. Academic, New York
30. Adamo C, Barone V (1998) J Chem Phys 108:664–675
31. Dunning THJ (1989) J Chem Phys 90:1007–1023
32. Li Q, Yin P, Liu Y, Tang AC, Zhang H, Sun Y (2003) Chem Phys Lett 375:470–476
33. Yao XQ, Hou XJ, Jao H, Xiang HW, Li YW (2003) J Phys Chem A 107:9991–9996
34. Miles AJ, Wien F, Lees JG, Rodger A, Janes RW, Wallace BA (2003) Spectroscopy 17:653–661